



Carbon footprint assessment in manufacturing Industry 4.0 using machine learning with intelligent Internet of things

Zhao Liu¹ · Gangying Yang¹ · Yi Zhang¹

Received: 14 June 2023 / Accepted: 15 August 2023

© The Author(s), under exclusive licence to Springer-Verlag London Ltd., part of Springer Nature 2023

Abstract

One important application area for sensor data analytics is Industry 4.0. Industrial furnaces (IFs) are sophisticated devices utilised in industrial production applications that need for unique heat treatment cycles. They are built with specialised thermodynamic materials and methods. emission of black carbon (EoBC) during IF operation as a result of the incomplete combustion of fossil fuels is one of the most important problems. This research proposes novel technique in carbon footprint analysis in environmental data from green manufacturing Industry 4.0 using machine learning with intelligent Internet of things (IIoT). Here, the environmental data from green manufacturing industry is collected and processed for analysing the presence of carbon by air monitoring by hidden fuzzy Gaussian kernel-based principle analysis. The experimental analysis is carried out for various air-monitored data in terms of training accuracy, positive predictive value, precision, robustness, energy consumption. Finally, we suggest ways for reducing carbon emissions and energy usage based on case studies that make use of our methodology. By making accounting simpler, we intend to encourage further investigation into energy-efficient algorithms and advance the long-term development of machine learning studies.

Keywords Carbon footprint analysis · Green manufacturing · Industry 4.0 · Air monitoring · Machine learning · IIoT

1 Introduction

The challenges related to global warming have now spread to all countries. According to Intergovernmental Panel on Climate Change (IPCC), scientists are over 95% positive that rising greenhouse gas concentrations as well as other anthropogenic activities are the primary responsible for the majority of the world's warming [1]. Burning fossil fuels for transportation, heating, and electricity production results in the global emission of about eight billion tonnes of carbon each year in the form of CO₂ [2]. The remaining products of the combustion of water (H₂O) and carbon monoxide (CO), also known as carbon dioxide (CO₂), a greenhouse gas, are emissions of carbon dioxide. The term “carbon footprint” is used as a benchmark for calculating CO₂ emissions [3]. The issue of honest and impartial quantitative measurement of ESG success in the area of environmental protection persists despite the ESG agenda's growing importance. Since cloud

computing already consumes 1% of the world's electricity and is expected to increase [4], this has major implications for the IT sector. Today's IT business heavily relies on artificial intelligence (AI) and machine learning (ML), two fast developing technologies with enormous potential for disruption. AI and ML have the potential to reduce environmental issues and human-caused harm in a variety of ways. In example, they could be used to produce and handle vast amounts of interconnected data in order to more thoroughly understand Earth and forecast environmental behaviour under diverse conditions. This might deepen our comprehension of environmental processes and enable us to take better judgements. Additionally, it is possible to simulate the effects of destructive activities like deforestation, soil erosion, flooding, and an increase in greenhouse gases in atmosphere using AI and ML [5]. In the end, these technologies have enormous potential to advance our comprehension and management of the environment.

As part of the idea of “Green AI”, several AI-based solutions are being developed to attain carbon neutrality. Decrease of greenhouse gas (GHG) emissions is the ultimate goal of these methods. In truth, artificial intelligence (AI) can contribute to lessening effects of climate issue, for

✉ Yi Zhang
Yi_zhang5@outlook.com

¹ School of Economics and Management, Guizhou Institute of Technology, Guiyang 550003, China

instance by designing smart grids, creating low-emission infrastructure, and modelling climatic changes. Nevertheless, it is also essential to take into consideration CO₂ emissions that AI itself produces as a result of learning as well as using AI methods. In actuality, AI advances to bigger as well as bigger methods with rising computational complexity, which leads to increased electrical energy use and, ultimately, equivalent carbon emissions (eq. CO₂) [6].

2 Related works

Several publications, notably [7], have modelled the COVID-19 transmission period's worldwide CO₂ emission footprint. The majority of existing works either have a partial or local context, as in [8] China, [9] wheat fields, or [10] paddy fields in India, or [11] Turkish transportation, where the modelling parameters and methodology are inappropriate for predicting global CO₂ emissions. Below, in chronological order, are the advantages and drawbacks of the local works that are currently available. ML and artificial neural network-based modelling were used to anticipate local CO₂ emissions for the case of the Iranian domain in [12]. The CO₂ emissions from manufacture of cement and fossil fuels are shown in [13]. A local Chinese county named Changxing served as the basis for CO₂ driver and emission forecasts in [14]. Additionally, ref. [15] uses data from the Indian subcontinent for the years 1995 to 2018 to analyse and predict CO₂ emissions. The Arabian region's CO₂ emissions are shown in [16]. [17] explains how CO₂ emissions in the Chinese region work in concert to reduce PM2.5 emissions. Furthermore, while ref. [18] offers a good summary of CO₂ emission and related difficulties, it falls short in terms of developing a CO₂ emission method for a global scenario. The model created by the IPCC provides the most precise CO₂ predictions to date. Producing goods with low emissions is crucial as well as demonstrating several aspects of new items reduced carbon footprint. Though they are not frequently utilised in management of production lines, ML techniques have lately been applied in the evaluation of supply chains. The carbon footprint of lettuce cultivation is evaluated in [17], which also discusses vegetable production. In PAS 2050, explicit explanations and examples of the use of life cycle assessment (LCA) in CF evaluations are provided. [19] contains a discussion along these lines. There are no many papers that discuss LCA assessment in relation to frozen vegetable business or the food processing industry. Holloway and Mengersen analyse how statistical techniques for remote sensing can be used in sustainable processes in [20]. Authors of [21] examine CF of a production line for veggie burgers. The use of ML techniques in the manufacture of frozen vegetables is demonstrated in [22], where the authors employ classification techniques such as support vector machines, random forests, and multilayer

perceptrons to evaluate the production process using their expert knowledge.

3 Proposed model

Figure 1 illustrates how the energy consumption in this study, which includes the burning of coal and electrical energy, directly increases CO₂ emissions. Data on energy use were gathered from Yogyakarta, Indonesia's alcohol industry. The information on energy consumption is taken from historical data that was utilised in the production process, including the amount of electrical energy consumed throughout production process in kWh and the amount of coal burned in kg.

The statistics for electrical energy use and coal burning must be converted into kilogrammes of CO₂ (kgCO₂). The value of electrical emission factor relates to emission factors that Perusahaan Listrik Negara (PLN) has set. PLN is a government-owned corporation that manages all facets of power in Indonesia. Electricity's emission factor, which is 0.725 kg/kWh, is worth. Equation 1 illustrates how to convert electrical energy by multiplying quantity of energy utilised by calorific value or emission factor.

$$E_{CO_2}^E = \sum_{t=1}^t A_{(E)t} \times F_{(E)t} \quad (1)$$

where $t = 1$.

Quantity of CO₂ emissions produced by burning coal and other fossil fuels is thus dependent on a number of factors. While fuel kinds are indicated by emission factors, fuel quantity is represented as activity data. Eqs. (2)–(5) provide the main equation utilised to evaluate CO₂ emissions from coal.

$$E_{CO_2}^F = C_x E F \quad (2)$$

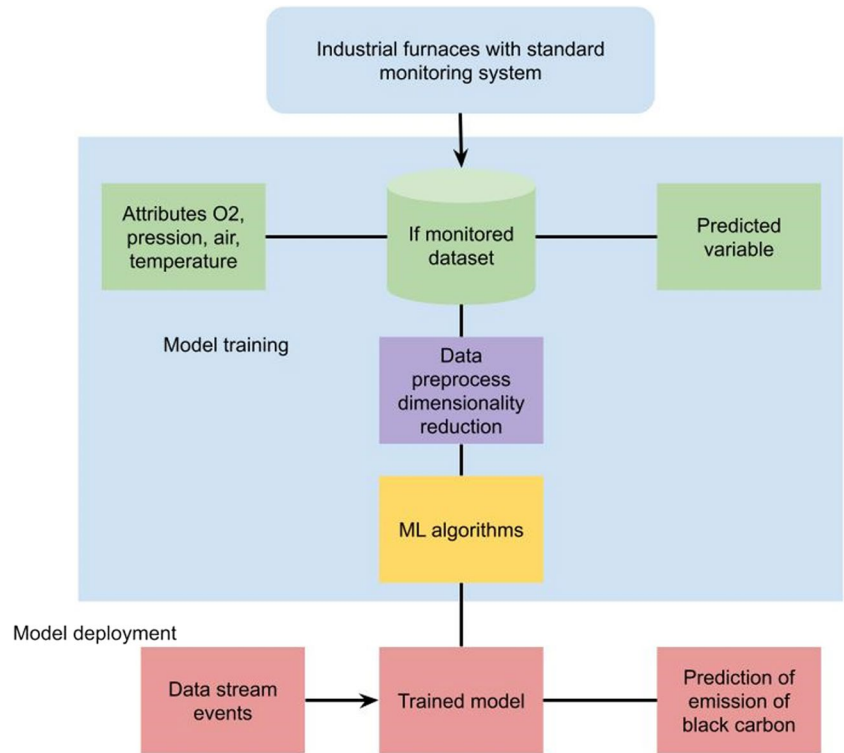
$$E_{CO_2}^F = \text{CO}_2 \text{ emission from combusted fuel (kg} \cdot \text{CO}_2) \quad (3)$$

We aim to develop some statistical models that will allow us to establish with certainty which factors are having a significant influence on the emission of greenhouse gases. It is important to understand that the objective of this study, which is to determine independent factors that collectively influence dependent variable, or the levels of CO₂ emissions across the entire cross-sectional data, among the three emission groups, is to determine the CO₂ emission values.

3.1 Air monitoring by hidden fuzzy Gaussian kernel based principle analysis

A vector of L dimensions is implied by the indicator u , which is defined as $u = [u_1, u_2, \dots, u_L]$ [$u_0 T, u_1 T, \dots, u_{MT}$], where $u_m T = [u_1 m, u_2 m, \dots, u_N m]$ and $unm [0,1]$ denotes the probability of $\text{Pr}(x_{nm} = 1)$. By learning the parameter u , it is

Fig. 1 proposed carbon footprint analysis



possible to determine (x, u) when this strategy is used. Additionally, X is vectorized as follows: $x = [x_0, 1_T, x_{MT}]$, where $x_{MT} = [x_{1m}, x_{2m}, \dots, x_{Nm}]$. The distribution function (x, u) under the Bernoulli distribution is normalized as Eq. (6):

$$(x, u) = \prod_{l=1}^L u_l x_l (1-u_l) = 1(1-u_l)(1-u_l). \quad (6)$$

An initial process connects to top CAP according to Eq. (8). Therefore, the likelihood of an operation being connected with alternate CAPs is 0 when it is assigned to CAP. A single sample is split into $M + 1$ autonomous blocks, x_0, x_1, x_M , and it is connected to the CPU. Valuable samples are gathered in T , sampling is done according to T 's cardinality, which is implied by the symbol $|T|$, and S is the result. It shows that the closer to (x) and (x) are, the smaller the minimum (q, p) is. It shows Eq. (7) as follows:

$$\min H(q, p) = \max \sum q(x) \ln p(x) = \max \frac{1}{S} \sum \ln p(x, u), \quad (7)$$

The objective is utilised to determine the best optimal indicator u for lowering (q, p) based on problems in Eq. (10). In the t th iteration, a candidate is chosen from S series of random examples and retrieved using the probability (x, u) . Adaptive sampling's potential sample is established. Then, elite samples are chosen, such as x [1, 2], or [elite], which offers the lower aim. Then, Eq. (8) is used to get best indicator u for strategy x .

$$u^* = \arg \max_u \frac{1}{S} \sum_{s=1}^{-S_{elite}} \ln p(x^{[s]}, u) \quad (8)$$

$$u_l^* = \frac{1}{S_{elite}} \sum_{s=1}^{S_{elite}} x_l^{[s]} \quad (9)$$

The CE-related measure from the model that is now being given is used to increase the probability. Function $u(t+1)$ is improved in $(t+1)$ th iteration based on the assumption that sampling is random as well as sample count is minimum. This is managed by Eqs. (8) and (9), and it applies by Eq. (10).

$$u^{(t+1)} = \alpha u^* + (1 - \alpha) u^{(t)} \quad (10)$$

where the learning value is implied by $[0, 1]$. For a CE-aided model, iterations typically converge on the best optimised solution to problems.

$$A' = \left\{ (x, \mu), \mu_{A'}(x, \mu) \mid \forall x \in U, \mu \in [0, 1] \right\} \quad (11)$$

It is easy to create type-II fuzzy sets by first creating a type-I set and giving each element a lower and upper membership degree to create footprint of uncertainty (FOU), or range between lower as well as upper membership values. It is possible to define a type-II fuzzy set as Eq. (12).

$$A' = \{ (x, \mu_U(x), x, \mu_L(x)) \mid \mu_L(x) \leq \mu(x) \leq \mu_U(x), \mu_L(x) = [\mu(x)]^\alpha, \mu \in [0, 1] \} \quad (12, 13)$$

$$\mu_U(x) = [\mu(x)]^{\frac{1}{\alpha}} \quad (14)$$

where $\alpha \in (1, \infty)$. Sigmoid activation function is a popular activation function in multilayer perceptrons. For binary classification issue, sigmoid function produces continuous values in range $[0, 1]$ that indicate likelihood of each class. Sigmoid function allows NN to learn more complicated characteristics because it introduces non-linearity in hidden layers (Eq. (15)).

$$\text{sig}(x) = \frac{1}{1 + e^{-x}} \quad (15)$$

$$\varphi_L(x) = \left[\frac{1}{1 + e^{-x}} \right]^{\alpha} \quad (16)$$

Equation (17) defines suggested fuzzy gradient descent as follows:

$$\mathbf{w} = \mathbf{w} - \text{mean}(|\mathbf{u}_1 - \mathbf{u}_2|^2) \times \eta \times \frac{d}{d\mathbf{w}} \varphi \quad (17)$$

$$\eta(\pi) = \mathbb{E}_{s_0, a_0, \dots} \left[\sum_{t=0}^{\infty} \gamma^t r(s_t) \right], \text{ where} \quad (18)$$

$$s_0 \sim \rho_0(s_0), a_t \sim \pi(a_t | s_t), s_{t+1} \sim P(s_{t+1} | s_t, a_t) \quad (19)$$

$$Q_{\pi}(s_t, a_t) = \mathbb{E}_{s_{t+1}, a_{t+1}, \dots} \left[\sum_{l=0}^{\infty} \gamma^l r(s_{t+l}) \right] \quad (20)$$

$$V_{\pi}(s_t) = \mathbb{E}_{a_t, s_{t+1}, \dots} \left[\sum_{l=0}^{\infty} \gamma^l r(s_{t+l}) \right] \quad (21)$$

$$A_{\pi}(s, a) = Q_{\pi}(s, a) - V_{\pi}(s), \text{ where} \quad (22)$$

$$a_t \sim \pi(a_t | s_t), s_{t+1} \sim P(s_{t+1} | s_t, a_t) \text{ for } t \geq 0. \quad (23)$$

$$\eta(\tilde{\pi}) = \eta(\pi) + \mathbb{E}_{s_0, a_0, \dots, \tilde{\pi}} \left[\sum_{t=0}^{\infty} \gamma^t A_{\pi}(s_t, a_t) \right]_1 \quad (24)$$

$$\rho_{\pi}(s) = P(s_0 = s) + \gamma P(s_1 = s) + \gamma^2 P(s_2 = s) + \dots, \quad (25)$$

$$\begin{aligned} \eta(\tilde{\pi}) &= \eta(\pi) + \sum_{t=0}^{\infty} \sum_s P(s_t = s | \tilde{\pi}) \sum_a \tilde{\pi}(a | s) \gamma^t A_{\pi}(s, a) \\ &= \eta(\pi) + \sum_s \sum_{t=0}^{\infty} \gamma^t P(s_t = s | \tilde{\pi}) \sum_a \tilde{\pi}(a | s) A_{\pi}(s, a) \\ &= \eta(\pi) + \sum_s \rho_{\tilde{\pi}}(s) \sum_a \tilde{\pi}(a | s) A_{\pi}(s, a). \end{aligned} \quad (26)$$

$\sum_a \tilde{\pi}(a | s) A_{\pi}(s, a) < 0$ It is challenging to directly optimise Eq. (25) due to complicated dependence of $\rho_{\tilde{\pi}}(s)$ on $\tilde{\pi}$. The structures of the 13 acquired retinoblastomas indicate that proposed method is more effective than actual image. Tumours that overlap are correctly classified and mapped to

the source node. The formation of the tumour's structure is similar to that of the image of the ground truth by Eq. (27).

$$L_{\pi}(\tilde{\pi}) = \eta(\pi) + \sum_s \rho_{\pi}(s) \sum_a \tilde{\pi}(a | s) A_{\pi}(s, a). \quad (27)$$

$$L_{\pi_{\theta_0}}(\pi_{\theta_0}) = \eta(\pi_{\theta_0}) \quad (28)$$

$$\nabla_{\theta} L_{\pi_{\theta_0}}(\pi_{\theta}) \Big|_{\theta=\theta_0} = \nabla_{\theta} \eta(\pi_{\theta}) \Big|_{\theta=\theta_0} \quad (29)$$

Each of them has benefits and drawbacks, but given the topic under study and the requirements for creating a measuring model for grant-funded projects, we thought it was appropriate to adopt some features from each model and incorporate additional problems from other methodologies in order to create a model that was straightforward to use while also producing reliable results. The low pace at which EU funds are being utilised, the low volume of public awareness campaigns about the issues brought on by GHG emissions, the dearth of national scientific research and publications in this area, and the uncertain outcomes of the Kyoto Protocol commitment. As a result, we provide a simple methodology that can be used by any prospective grant applicant to calculate the carbon impact of investment projects. The model should incorporate a variety of predetermined scenarios, options, and data. Once applicants have realised how important it is to consider the potential impact of a project's design on the climate, the model's complexity should gradually increase while also taking advantage of fresh research findings and globally accepted standards. The project-centred technique used for carbon footprint analysis during the project's implementation phase is used rather than the institution- or organisation-centred approach. As a result, we are compiling an inventory of specific actions that might take place while the project is being implemented. Regardless of the project's kind or the activity engaged, the approach for calculating the carbon footprint during the implementation phase will be used for all projects. A grant-funded project's primary activities typically include administrative tasks like project management, purchasing, informational campaigns, and publicity; purchasing of facilities and equipment; receiving, installing, and commissioning of equipment; and construction projects like upgrades, additions, and new construction. The building activities are one of the three primary types of activities that should be taken into account in terms of emissions produced.

If equipment is imported and shipped a long way, the purchase process may produce large emissions. Due to the fact that supply contracts are typically signed after an acquisition process, when it is important to uphold the concept of competition by allowing unlimited access to any possible tender in the procedure, the suppliers and their locations are

unknown during the pre-implementation period. The same principle must be observed when purchasing construction projects and materials, but the idea of doing so is accepted in international practise due to the challenges involved in transporting large quantities of material over great distances and the lower prices offered on the local market. Therefore, even if a foreign company is hired to perform construction work, it is usually more cost-effective to use public funds to buy building supplies from the local market. For a certain kind of product, businesses, however, frequently employ a fewer number of procedures. Due to this reality, our study's next phase will focus on developing and using a method to control production using a minimal number of procedures. We demonstrated how good process management, such as increasing average power as well as output capacity, can lead to decreased energy consumption per tonne of finished product. Figure 2 depicts general layout of statistics as well as ML techniques.

4 Results and discussion

The variables with highest absolute correlation coefficient as well as lowest absolute significance coefficient were age, mean depth, and NPP0. Additionally, sample size that is now available is sufficient, and previous research have found a significant influence from latitude. Latitude is consequently considered as an input as well, and reasoning is tested via sensitivity analysis. Since these components are obviously distinct from one another, it is not necessary to look into their relationship. Only reservoirs with current as well as accessible records for four parameters would use this collection of data. After removing the inaccurate data, a dataset of 251 data points was used for simulation.

4.1 Dataset description

In this study, majority of the CO₂ emission fluxes from the reservoir surface were based on data collection. In some recent articles, CO₂ emission monitoring data from reservoirs was also assembled. Some of missing values for numerous important reservoir as well as monitoring specifications that were acquired from relevant literature [17] were filled in utilising GRand database. Another important statistic, NPP0 near reservoir, was extracted from map of HANPP. The 10 metrics we compiled for 235 reservoirs with a global distribution were latitude, age, chlorophyll-a, MD, RT, DOC, TP, NPP0 and CO₂ flux. CO₂ flux served as method output in this study. Table 1 includes minimum, maximum, mean, median, standard deviation, and variation coefficient among its statistical properties.

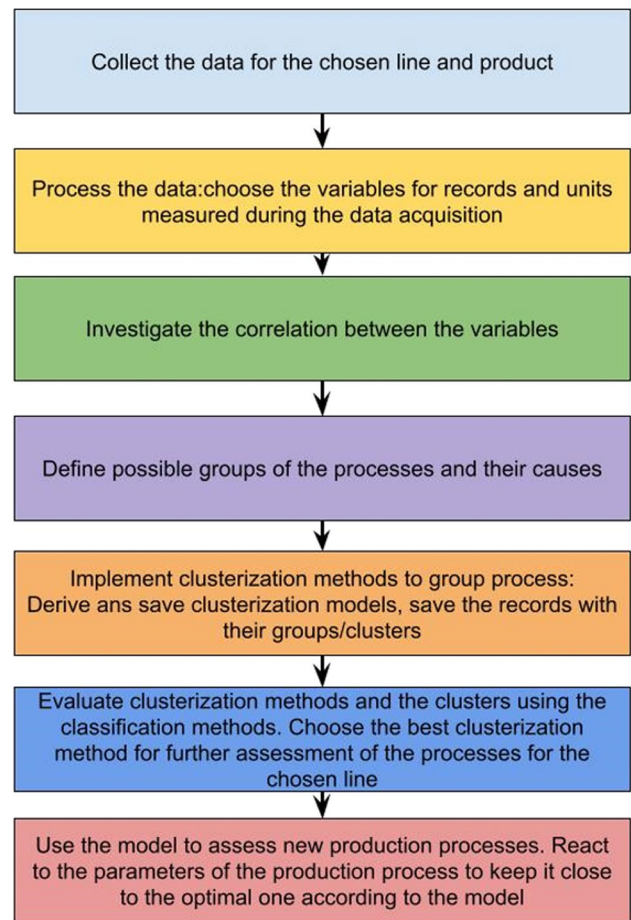


Fig. 2 General outline of product assessment

They used IPCC recommendations for national GHG inventories to determine amount of global GHG emissions produced by manufacture of synthetic N fertiliser, transportation, and agricultural usage. Using the activity data they gathered and the necessary EFs, they correspondingly computed the emissions at the national level. Each is expected to make up one-third of the total, with indirect emissions making up about two-thirds.

Table 2 shows comparison for various carbon datasets. Here, datasets analysed are GRand, NPP0, and HANPP in terms of training accuracy, positive predictive value, precision, robustness, and energy consumption.

Figure 3 shows the comparative analysis for training accuracy. Here, it shows the proposed technique training accuracy of 92%, existing LCA 91%, ML 92% for GRand dataset; then for NPP0 dataset proposed technique training accuracy of 93%, existing LCA 91%, ML 92%; and proposed technique training accuracy of 95%, existing LCA 91%, ML 93% for HANPP dataset.

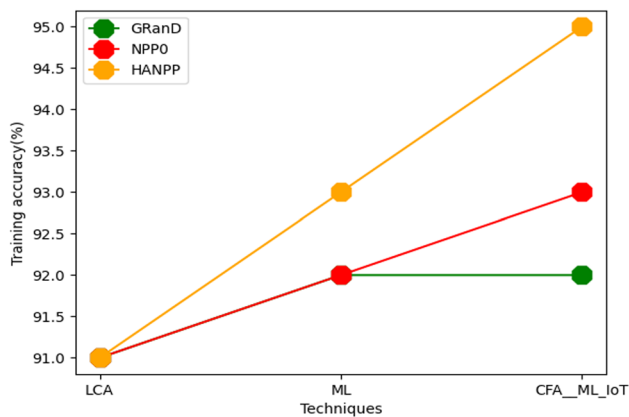
In Figure 4, the comparative analysis for positive predictive value is shown. Here, it shows the proposed technique

Table 1 Statistical specifications for datasets

Parameters	Unit	Max	Min	Mean	SD	Median	VC
Lat		68.00	−42.93	31.96	26.36	38.17	0.83
Age	yrs	95.00	1.00	39.09	24.55	36.00	0.63
Chl-	μL^{-1}	137.50	0.20	12.03	24.78	4.13	1.96
WT	C	35.00	6.30	17.88	5.52	17.40	0.30
MD	m	400.00	0.30	26.58	40.26	15.00	1.52
RT	days	13,140.00	1.25	665.75	1689.54	180.00	2.54
DOC	mgL^{-1}	30.00	1.25	4.79	4.01	3.82	0.84
TP	HgL^{-1}	500.00	1.40	62.61	96.89	29.00	1.55
NPPO	$\text{mgCm}^{-2}\text{d}^{-1}$	3200.68	151.90	1529.21	604.70	1574.50	0.40
CO flux	$\text{mgCm}^{-2}\text{d}^{-1}$	3800.00	−356.00	400.90	569.89	254.75	1.42

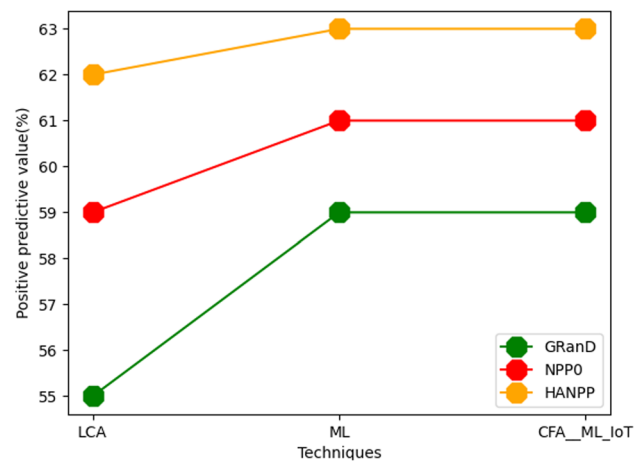
Table 2 Analysis based on various carbon elements dataset

Dataset	Techniques	Training accuracy	Positive predictive value	Precision	Robustness	Energy consumption
GRanD	LCA	91	55	89	51	59
	ML	92	59	92	53	62
	CFA__ML_IoT	92	59	93	55	63
NPP0	LCA	91	59	91	55	59
	ML	92	61	93	58	64
	CFA__ML_IoT	93	61	95	59	65
HANPP	LCA	91	62	92	55	65
	ML	93	63	94	59	66
	CFA__ML_IoT	95	63	97	62	68

**Fig. 3** Comparison of training accuracy

positive predictive value of 59%, existing LCA 55%, ML 59% for GRanD dataset; then for NPP0 dataset proposed technique positive predictive value of 61%, existing LCA 61%, ML 59%; and proposed technique positive predictive value of 63%, existing LCA 62%, ML 63% for HANPP dataset.

Figure 5 shows analysis for precision. Here, it shows the proposed technique precision of 93%, existing LCA 89%,

**Fig. 4** Comparison of positive predictive value

ML 92% for GRanD dataset; then for NPP0 dataset proposed technique precision of 95%, existing LCA 91%, ML 93%; and proposed technique precision of 97%, existing LCA 92%, ML 94% for HANPP dataset.

In Fig. 6, the analysis for robustness is shown. Here, it shows the proposed technique robustness of 55%, existing

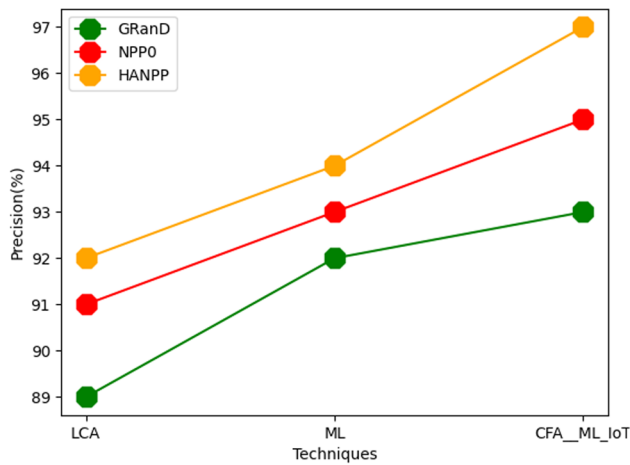


Fig. 5 Comparison of precision

LCA 51%, ML 53% for GRanD dataset; then for NPP0 dataset proposed technique robustness of 59%, existing LCA 55%, ML 58%; and proposed technique robustness of 62%, existing LCA 55%, ML 59% for HANPP dataset.

Figure 7 shows analysis for energy consumption. Here, it shows the proposed technique energy consumption of 63%, existing LCA 59%, ML 62% for GRanD dataset; then for NPP0 dataset proposed technique energy consumption of 65%, existing LCA 59%, ML 64%; and proposed technique energy consumption of 68%, existing LCA 65%, ML 66% for HANPP dataset.

Through analyses of their learning curves, the predictive models' performance over experience is evaluated in this section. A method utilised in ML to interpret method behaviour is learning curve. Predictive methods can occasionally exhibit either overfitting or underfitting. Learning-curve method in our case study is useful in this regard to find differences between

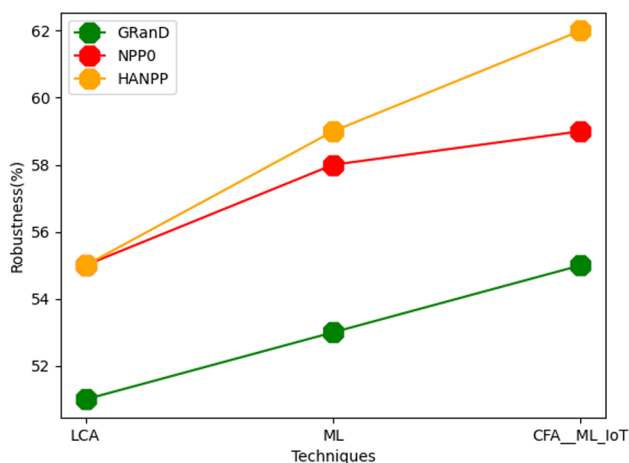


Fig. 6 Comparison of robustness

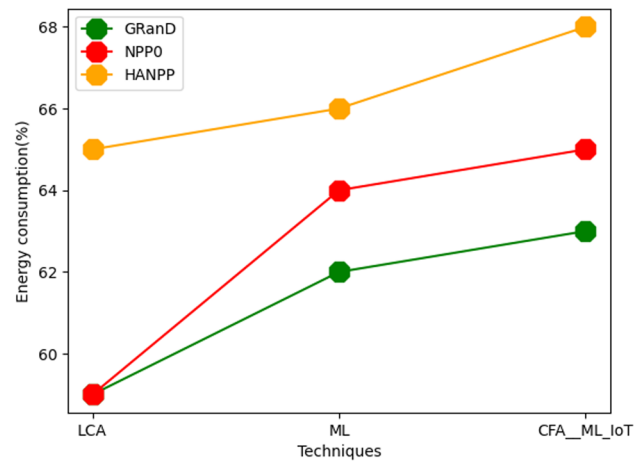


Fig. 7 Comparison of energy consumption

the four predictive models compared. Both the training and validation faults are displayed by the learning curve. Cross-entropy loss function, often known as log loss, is the error measure that is most frequently employed for binary classification. We started the training size with 50 samples for assessment purposes and then gradually expanded the size by 50 at a time. The log loss was calculated at each stage and a 10-fold cross validation was taken into account.

Walls and centre are about 0.40 m and 0.60 m long, respectively. Both the greenhouse for forced convection (GDFC) and the greenhouse for natural convection drying (GDNC) were used for the trials. On the GDNC roof, a 0.0722 m² air gap developed. As a result, the thermophysical actions brought on by the air gap removed the moisture from the product. A fan positioned on side wall of drying chamber with an air speed of 2.4 m/s was used to remove moisture from product during forced drying. To force a drying process, the air gap was sealed. The substance to be dried was determined to be grape. In the literature, it is said that grapes take a long time to dry out in the sun [39]. However, using a machine-learning algorithm to model necessitates a vast amount of data. This is due to the model's decreasing error rate, which is caused by the growing amount of data. Because they take so long to dry, grapes were chosen. As a result, more information was gathered, and a more effective model was created. The items were placed on a mesh tray and air was allowed to enter greenhouse from side of drying chamber dispersal.

5 Conclusion

This study suggests a brand-new machine learning method for detecting carbon footprints in the manufacturing sector. These elements are included in the suggested strategy as part

of our ongoing work on an advanced optimisation method to create new paradigms for operations as well as safety measures targeted at improving capabilities of organisations. This study is first to describe ML techniques in estimating black carbon emissions in industrial furnaces through real data analysis, a topic that has largely gone untapped. Similar to this, we want to evaluate predictive models in further real-world applications with more case studies in fields like production time optimisation, fuel and gas optimisation, and industrial furnace model optimisation, among others. Concepts presented in this research will encourage researchers as well as practitioners to develop more predictive methods to improve business value of industrial organisations so that we can benefit from ML concepts that support materialisation of Industry 4.0 concepts.

Funding This work was supported by the Academic Seedlings and Exploration-Innovation Project of Guizhou Institute of Technology, Study on carbon information disclosure and carbon trading quota mechanism of industrial enterprises in Guizhou Province. (GZLGXM-25).

Data availability All the data are available in the manuscript.

Declarations

Ethics approval This article does not contain any studies with animals performed by any of the authors.

Conflict of interest The authors declare no competing interests.

References

- Wang A, Hu S, Li J (2022) Using machine learning to model technological heterogeneity in carbon emission efficiency evaluation: the case of China's cities. *Energy Econ* 114:106238
- Zhao J, Kou L, Wang H, He X, Xiong Z, Liu C, Cui H (2022) Carbon emission prediction model and analysis in the Yellow River basin based on a machine learning method. *Sustain* 14(10):6153
- Selvan R, Bhagwat N, Wolff Anthony LF, Kanding B, Dam EB (2022) Carbon footprint of selecting and training deep learning models for medical image analysis. In: *Medical Image Computing and Computer Assisted Intervention—MICCAI 2022: 25th International Conference, Singapore, September 18–22, 2022, Proceedings, Part V*. Springer Nature Switzerland, Cham, pp 506–516
- Rubio-Loyola J, Paul-Fils WRS (2022) Applied machine learning in industry 4.0: case-study research in predictive models for black carbon emissions. *Sensors* 22(10):3947
- Hu Y, Man Y (2023) Energy consumption and carbon emissions forecasting for industrial processes: status, challenges and perspectives. *Renew Sust Energ Rev* 182:113405
- Lin X, Ma J, Chen H, Shen F, Ahmad S, Li Z (2022) Carbon emissions estimation and spatiotemporal analysis of china at city level based on multi-dimensional data and machine learning. *Remote Sens* 14(13):3014
- Gao P, Zhu C, Zhang Y, Chen B (2023) An approach for analyzing urban carbon emissions using machine learning models. *Indoor Built Environ*. <https://doi.org/10.1177/1420326X231162253>
- Dong H, Zhang L (2023) Transition towards carbon neutrality: Forecasting Hong Kong's buildings carbon footprint by 2050 using a machine learning approach. *Sustain Prod Consum* 35:633–642
- Shahzad U, Sengupta T, Rao A, Cui L (2023) Forecasting carbon emissions future prices using the machine learning methods. *Ann Oper Res* 1–32. <https://doi.org/10.1007/s10479-023-05188-7>
- Bhatt H, Davawala M, Joshi T, Shah M, Unnarkat A (2023) Forecasting and mitigation of global environmental carbon dioxide emission using machine learning techniques. *Clean Chem Eng* 5:100095
- Chiu MC, Tu YL, Kao MC (2022) Applying deep learning image recognition technology to promote environmentally sustainable behavior. *Sustain Prod Consum* 31:736–749
- Luccioni AS, Hernandez-Garcia A (2023) Counting carbon: a survey of factors influencing the emissions of machine learning. *arXiv preprint arXiv:2302.08476*
- Peng H, Lu Y, Gupta S, Wang Q (2022) Dynamic and heterogeneity assessment of carbon efficiency in the manufacturing industry in China: Implications for formulating carbon policies. *Environ Impact Assess Rev* 97:106885
- Ahmed M, Shuai C, Ahmed M (2022) Influencing factors of carbon emissions and their trends in China and India: a machine learning method. *Environ Sci Pollut Res* 29(32):48424–48437
- Ma Y, Liu H, Wang S (2023) Nonparametric approaches for analyzing carbon emission: from statistical and machine learning perspectives. *arXiv preprint arXiv:2303.14900*
- Aamir M, Bhatti MA, Bazai SU, Marjan S, Mirza AM, Wahid A et al (2022) Predicting the environmental change of carbon emission patterns in South Asia: a deep learning approach using BiLSTM. *Atmosphere* 13(12):2011
- Rafat K, Islam S, Mahfug AA, Hossain MI, Rahman F, Momen S et al (2023) Mitigating carbon footprint for knowledge distillation based deep learning model compression. *PLoS One* 18(5):e0285668
- Czarnecki S, Hadzima-Nyarko M, Chajec A, Sadowski Ł (2022) Design of a machine learning model for the precise manufacturing of green cementitious composites modified with waste granite powder. *Sci Rep* 12(1):13242
- Sun W, Huang C (2022) Predictions of carbon emission intensity based on factor analysis and an improved extreme learning machine from the perspective of carbon emission efficiency. *J Clean Prod* 338:130414
- Zhou Y, Xia Q, Zhang Z, Quan M, Li H (2022) Artificial intelligence and machine learning for the green development of agriculture in the emerging manufacturing industry in the IoT platform. *Acta Agric Scand - B Soil Plant Sci* 72(1):284–299
- Ouadi H, Laalam A, Hassan A, Chemmakh A, Rasouli V, Mahmoud M (2023) Design and performance analysis of dry gas fishbone wells for lower carbon footprint. *Fuels* 4(1):92–110
- Tirth V, Algahtani A, Alghtani AH, Al-Mughanham T, Irshad K (2023) Sustainable nanomaterial-based technologies for renewable energy production and efficient storage based on machine learning techniques. *Sustain Energy Technol Assess* 56:103085

Publisher's note Springer Nature remains neutral with regard to jurisdictional claims in published maps and institutional affiliations.

Springer Nature or its licensor (e.g. a society or other partner) holds exclusive rights to this article under a publishing agreement with the author(s) or other rightsholder(s); author self-archiving of the accepted manuscript version of this article is solely governed by the terms of such publishing agreement and applicable law.